Defective Formation of the Inner Limiting Membrane in Laminin β2- and γ3-Null Mice Produces Retinal Dysplasia

Germán Pinzón-Duarte,[1] *Gerard Daly,*[1] *Yong N. Li,*[2] *Manuel Koch,*[3] *and William J. Brunken*[1,2,4]

Purpose. Retinal basement membranes (BMs) serve as attachment sites for retinal pigment epithelial cells on Bruch's membrane and Müller cells (MCs) on the inner limiting membrane (ILM), providing polarity cues to adherent cells. The β2 and γ3 chains of laminin are key components of retinal BMs throughout development, suggesting that they play key roles in retinal histogenesis. This study was conducted to analyze how the absence of both β2- and γ3-containing laminins affects retinal development.

Methods. The function of the β2- and γ3-containing laminins was tested by producing a compound deletion of both the β2 and the γ3 laminin genes in the mouse and assaying the effect on postnatal retinal development by using anatomic and electrophysiological techniques.

Results. Despite the widespread expression of β2 and γ3 laminin chains in wild-type (WT) retinal BMs, the development of only one, the ILM, was disrupted. The postnatal consequence of the ILM disruption was an alteration of MC attachment and a resultant disruption in MC apical–basal polarity, which culminated in retinal dysplasia. Of importance, although their density was altered, retinal cell fates were unaffected. The laminin mutants have a markedly decreased visual function, resulting in part from photoreceptor dysgenesis.

Conclusions. These data suggest that β2 and γ3 laminin isoforms are critical for the formation and stability of the ILM. These data also suggest that attachment of the MC to the ILM provides important polarity cues to the MC and for postnatal retinal histogenesis. (*Invest Ophthalmol Vis Sci.* 2010;51:1773–1782) DOI:10.1167/iovs.09-4645

Laminins are extracellular matrix (ECM) glycoproteins composed of α, β, and γ subunits, which assemble into a single cruciform molecule. Five α, three β, and three γ laminin chains have been identified, forming 16 different isoforms.[1] Laminins bind to a variety of cell surface receptors, including integrins, dystroglycan, sulfated glycolipids, and syndecans. Laminins are key nucleating elements of the highly organized ECM known as BMs.[2,3] BMs and their receptors are indispensable during development, providing key polarity cues and conferring structural stability for macromolecular complexes by coupling the cytoskeleton to the ECM.[4,5] Several human diseases, including those of the central nervous system (CNS), which includes the eye, are linked to disruptions in laminin expression or deposition.[6–10]

In the CNS, at least three laminin isoforms have been identified: α3β3γ2, α4β2γ3, and α5β2γ3.[11] Both the β2 and γ3 laminin chains are present in retinal BMs (i.e., Bruch's membrane and the ILM). The temporal and spatial localization of β2 and γ3 laminin chains during development make them good candidates to participate in retinal histogenesis as organizing factors responsible for compartmentalization.[11] Therefore, to assess the function of β2- and γ3-containing laminins in development, we produced $\beta2^{-/-}\gamma3^{-/-}$ mice by gene ablation via homologous recombination, and we analyzed the retina. Retinal disruptions in the $\beta2^{-/-}\gamma3^{-/-}$ mice phenocopy some of the abnormalities described previously in the $\beta2^{-/-}\gamma3^{+/+}$ animal, such as perturbations in synaptogenesis and outer segment formation.[12] However, there are significant new aspects of the retinal phenotype in the $\beta2^{-/-}\gamma3^{-/-}$ retina that reveal roles for β2 and γ3 laminins in ILM synthesis and MC maturation. Specifically, the data presented suggest that β2- and γ3- containing laminins are critical for the proper assembly of the ILM and MC attachment to the ILM and that retinal lamination is dependent on adequate contact between the endfeet of MCs and an intact ILM. Disruptions in the integrity of the ILM lead to retinal dysplasia but not to alterations in terminal cell differentiation.

Materials and Methods

Animals

The animal procedures were in accordance with the institutional animal care and use committee and the ARVO Statement for the Use of Animals in Ophthalmic and Vision Research. Targeted mutations of the *Lamb2* and the *Lamc3* genes were produced to generate two independent lines of mice ($\beta2^{-/-}\gamma3^{+/+}$ and $\beta2^{+/+}\gamma3^{-/-}$, respectively).[13,14] These lines were crossed to generate homozygous, compound-null mutants ($\beta2^{-/-}\gamma3^{-/-}$). The animals were genotyped by PCR on genomic DNA derived from tail samples.[14] Mice with $\beta2^{+/+}\gamma3^{+/+}$, $\beta2^{-/-}\gamma3^{+/+}$, $\beta2^{+/+}\gamma3^{-/-}$, and $\beta2^{-/-}\gamma3^{-/-}$ genotypes were examined. The $\beta2^{-/-}\gamma3^{-/-}$ mice were smaller and died at a younger age, but did not display significant external morphologic defects; this failure to thrive is similar to that in the laminin β2-deficient mouse.[13] Before the tissue was collected, the animals were anesthetized with CO_2 and decapitated. Dissected retinas were examined

From the Departments of [1]Cell Biology and [4]Ophthalmology, State University of New York, Downstate Medical Center, Brooklyn, New York; the [2]Graduate Program in Molecular Cellular and Developmental Biology, Sackler School of Graduate Biomedical Sciences, Tufts University, Boston, Massachusetts; and the [3]Institute for Oral and Musculoskeletal Biology, Center for Biochemistry and Center for Molecular Medicine Cologne, University of Cologne, Cologne, Germany.

Supported by National Eye Institute Grant EY12676-09 (WJB), unrestricted funds from SUNY Downstate Medical Center, and a Deutsche Forschungsgemeinschaft (DFG) Grant SFB612 (MK B14).

Submitted for publication September 15, 2009; revised October 23, 2009; accepted October 30, 2009.

Disclosure: **G. Pinzón-Duarte**, None; **G. Daly**, None; **Y.N. Li**, None; **M. Koch**, P; **W.J. Brunken**, P

Corresponding author: William J. Brunken, SUNY Downstate Medical Center, Department of Cell Biology, 450 Clarkson Avenue, Box 5, Brooklyn, NY 11203; william.brunken@downstate.edu.

TABLE 1. Primary Antibodies

Cell Type	Antibody	Host	Source	Concentration	Reference
Used to identify retinal cells					
Rod photoreceptor	Rhodopsin	Clone RET-P1 monoclonal	Sigma-Aldrich, St. Louis, MO	1:500	15
Rod bipolar	αPKC	Clone MC5 monoclonal	Chemicon, Temecula, CA	1:500	16
Horizontal	Calbindin-D-28K	Mouse monoclonal	Sigma-Aldrich	1:500	16
Amacrine	Calretinin	Mouse monoclonal	Chemicon	1:500	16
Ganglion	Brn3a	Mouse monoclonal	Santa Cruz, Santa Cruz, CA	1:500	17
Müller	Glutamine synthetase	Goat polyclonal	Santa Cruz	1:500	16
	GFAP	Clone G-A-5 monoclonal	Chemicon	1:500	18
Used to detect basement membranes					
	Collagen IV	Rabbit polyclonal	Chemicon	1:100	19
	Laminin β2 chain	Rabbit polyclonal	Our laboratory	1:5,000	11
	Laminin γ3 chain	Rabbit polyclonal	Our laboratory	1:5,000	11
	Nidogen	Rabbit polyclonal	Ulrike Mayer*	1:3,000	19
	Pan-laminin	Rabbit polyclonal	Sigma-Aldrich	1:1,000	20
	Perlecan	Rat polyclonal	Santa Cruz	1:100,000	21
Used to detect basement membrane receptors					
	β-dystroglycan	Rabbit polyclonal	Dominique Mornet†	1:250	22

* Ulrike Mayer University of East Anglia, Norwich, UK.
† Université Montpellier, Montpellier, France.

by conventional histology, immunohistochemistry, and electron microscopy. To prevent confounding interpretation of the data, we matched eccentricity.

Conventional Light and Electron Microscopy

Postnatal day (P)7, P15, and P20 eyecups were immersed in ice-cold Karnovsky's fixative for 12 hours, postfixed in 2% glutaraldehyde and 1% osmium tetroxide for 1 hour, dehydrated, embedded in plastic, and sectioned. For an overview of the gross morphology, Nissl-stained 0.5-μm sections were used. Ultrathin sections were viewed and photographed on a transmission electron microscope (CM-10; Philips, Eindhoven, The Netherlands).

Immunohistochemistry

P15 retinas were used to assay neuronal cell differentiation, BM integrity, laminin, and β-dystroglycan expression. Postnatal day (P)10, P15, and P20 retinas were used to characterize MC maturation. The retinas were immersed for 30 minutes in ice-cold 4% paraformaldehyde, washed, cryoprotected, embedded (O.C.T. Compound; Finetek USA, Torrance, CA), and frozen. Radial sections (10 μm) were collected and incubated with primary antibodies (Table 1). Immunoreactions were visualized with Alexa (488 or 568)-conjugated secondary antibodies (1:500; Molecular Probes, Eugene, OR) and photographed (Eclipse E800 microscope; Nikon, Tokyo, Japan; with the Volocity suite of programs; Improvision Ltd., Lexington, MA).

Electroretinography

P18 wild-type (WT) and $\beta2^{-/-}\gamma3^{-/-}$ mice were dark-adapted for several hours and, in dim red light, anesthetized with 20 mg/kg ketamine HCl (Ketaset; Fort Dodge Animal Health, Fort Dodge, IA), followed by 65 mg/kg pentobarbital sodium (Nembutal; Ovation Pharmaceuticals Inc, Deerfield, IL). In a light-tight Faraday cage, visual responses were tested with 50-ms flashes; 10 flashes presented at a frequency of 0.5 Hz (PS22 Photopic stimulator; Grass Instruments, Quincy, MA) were averaged at a given stimulus intensity. For each animal, at least one set of recordings was made over a 4.4-log range of intensities, starting with the least bright flash. The responses were amplified (DAM 50 differential amplifier; World Precision Instruments, Sarasota, FL), recorded, and averaged (MacLab 8sp; AD Instruments, Mountain View, CA).

Cell-Surface Ligand Adhesion Assay

The rat Müller cell line (rMC-1, gift of Vijay P. Sarthy, Northwestern University, Evanston, IL),[23] is an SV40 large-T antigen–transformed cell line. After dissociation, single cell suspensions were plated onto different substrates (Table 2) in DMEM-F12 (Life Technologies Inc., Carlsbad, CA) medium in an atmosphere of 5% CO_2–balanced air at 37°C. After 2 hours, the cells were fixed in 4% paraformaldehyde in PBS for 20 minutes. The number of cells attached to each substrate was determined after staining with 0.1% cresyl violet.

RESULTS

Laminin β2 and γ3 Chains in ILM Development

In P15 WT retinas, β2 laminin immunoreactivity was observed in Bruch's membrane, the retinal blood vessels, and very strongly in the ILM (Fig. 1A). γ3-Laminin immunoreactivity had

TABLE 2. Protein Substrates for Adhesion Assays

Substrate	Source	Concentration
Recombinant full-length netrin-4	Our laboratory	10 μg/mL
Recombinant netrin-4 without C domain	Our laboratory	10 μg/mL
Recombinant laminin β2 short arm	Our laboratory	10 μg/mL
Engelbreth-Holm-Swarm sarcoma derived laminin	Invitrogen, San Diego, CA	10 μg/mL
Poly-L-lysine	Sigma-Aldrich, St. Louis, MO	100 μg/mL
Bovine serum albumin	Sigma-Aldrich	40 μg/mL

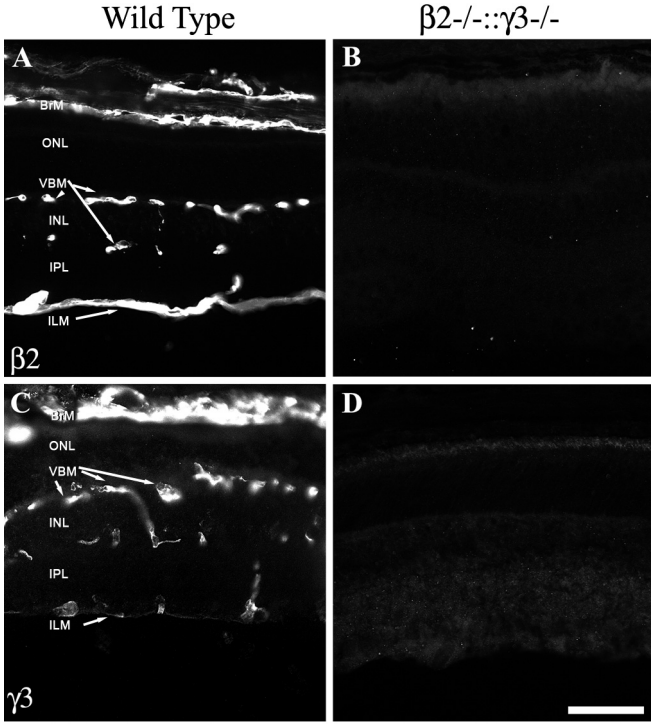

FIGURE 1. $\beta 2$ and $\gamma 3$ laminin expression was absent in mutant retinas. (**A**, **C**) P15 WT retina; (**B**, **D**) P15 laminin-deficient retina. (**A**) $\beta 2$ immunoreactivity was seen in all retinal BMs: Bruch's membrane, vascular BM, and the ILM. (**B**) This reactivity was completely absent in the mutant retina. (**C**) Strong deposition of $\gamma 3$ chain was found in Bruch's membrane and vascular BM, but it was weakly present in the ILM. (**D**) No $\gamma 3$ expression was seen in the mutant retina. Scale bar, 50 μm.

a similar distribution, albeit with more limited apparent deposition in the ILM (Fig. 1C). As expected, no immunolabeling was found for either the $\beta 2$ or the $\gamma 3$ chain in the compound-null animal (Figs. 1B, 1D), demonstrating that these animals were protein nulls. Similar results were obtained with Western blot (data not shown). To evaluate how the ablation of $\beta 2$ and $\gamma 3$ genes affect BM integrity, we examined the expression of canonical BM components in WT and mutant retinas (Table 1). In WT retinas, nidogen staining was observed as a thick, continuous band along the vitreal surface (i.e., the ILM), under the RPE (Bruch's membrane), and in the vascular BMs (Fig. 2A). In the $\beta 2^{-/-}\gamma 3^{+/+}$ retinas, nidogen staining in the ILM was largely intact; however, some spatial discontinuities were noted (Fig. 2B). In the $\beta 2^{+/+}\gamma 3^{-/-}$ retinas, the ILM was intact (Fig. 2C). In contrast, the $\beta 2^{-/-}\gamma 3^{-/-}$ retina was severely disrupted (Fig. 2D). Nidogen deposition was intact in the central retina (i.e., adjacent to the optic nerve head) but was completely absent over most of the vitreal surface. BM components (Table 1) in the retinal periphery were seen only in association with blood vessels (Fig. 2D, arrows; compare with perlecan in Fig. 7), suggesting that the ILM was absent from large regions of the $\beta 2^{-/-}\gamma 3^{-/-}$ retina. This effect was specific for ILM formation or stability, in that nidogen and perlecan deposition in other BMs, Bruch's membrane, vascular BMs, and extraocular muscle BMs (Fig. 2, arrowheads) was intact.

Disruptions in the ILM in the $\beta 2^{-/-}\gamma 3^{-/-}$ Retina

In the first postnatal week, although the general organization of the $\beta 2^{-/-}\gamma 3^{-/-}$ and WT retinas was similar (Figs. 3A, 3B), many abnormalities were evident in the $\beta 2^{-/-}\gamma 3^{-/-}$ retinas. In the outer retina, the OPL was thinned and the photoreceptor inner/outer segments were shorter. The inner plexiform layer (IPL) was considerably thinned (Fig. 3B), and the retinal ganglion cell (RGC) layer was disorganized, with many ectopic cells extruding into the vitreal cavity (Fig. 3B, arrows). During the second postnatal week, retinal lamination was progressively disrupted (Figs. 3C, 3D). Although large regions of the P15 mutant retinas appeared to have the normal laminar organization, the relative thickness of the different layers differed considerably across the retina. In addition, focal abnormalities with different degrees of severity were seen. The most prominent was the formation in the outer nuclear layer of photoreceptor rosettes that very often disrupted the subjacent layers (Fig. 3D). Also, ectopic photoreceptor cells were present in the subretinal space; their presence was spatially coupled to the disruptions of the OLM (see Fig. 8). In the INL, rosette-like clusters of cells composed of interneurons were found in every retina and were associated with ILM breakdown (not shown).

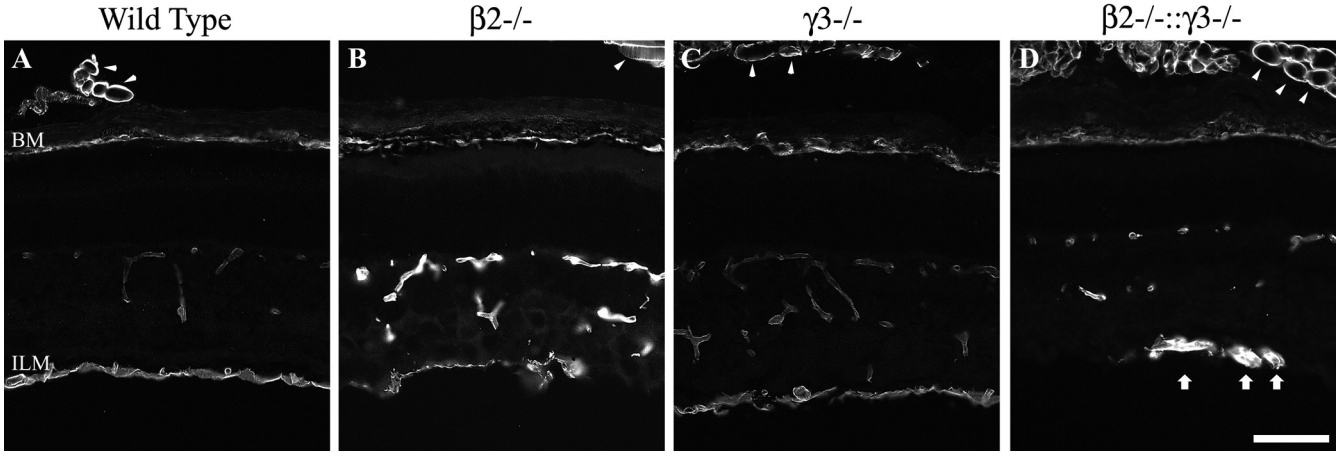

FIGURE 2. $\beta 2\gamma 3$ Laminin deletion produced differential disruption of the ILM. BMs were visualized with nidogen immunostaining in all genotypes (as indicated). (**A**) Nidogen staining was seen as a continuous band along both BM and the ILM; vascular BM was also labeled. The deposition of nidogen, in Bruch's membrane and the vascular BM, was intact in all genotypes. In contrast, the ILM organization was affected by laminin deletion. Nidogen deposition was largely normal in the $\gamma 3^{-/-}$ retina (**C**). In the $\beta 2^{-/-}$ retina, nidogen deposition was more punctate and there were limited regions of discontinuity (**B**). In the $\beta 2^{-/-}\gamma 3^{-/-}$ animals, nidogen deposition was largely lacking, with limited plaquelike staining associated with vitreal blood vessels (**D**, *arrows*). The extraocular muscle BM was intact in all genotypes (*arrowheads*). Scale bar, 50 μm.

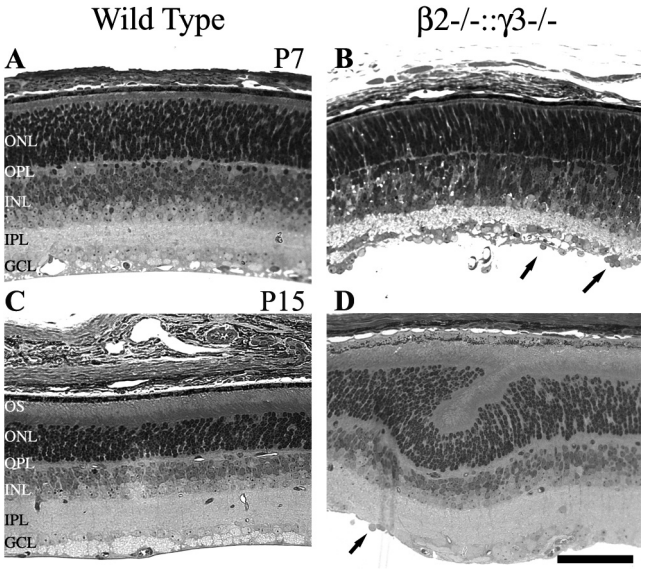

FIGURE 3. The retina became progressively dysplastic in the first 2 postnatal weeks. Radial sections through WT (**A**, **C**) and mutant retinas (**B**, **D**) at P7 (**A**, **B**) and P15 (**C**, **D**). At P7, the mutant retina showed some sign of developmental disruptions. The OPL was underdeveloped as were the outer and inner segments, the IPL thickness was reduced, and the RGC layer was disrupted, with numerous ectopic cells in the vitreous (*arrows*). At P15, retinal lamination was disrupted in discrete patches, and large rosettes were common in the mutant retina (**D**); in addition, ectopic clusters of cells were present in the INL (not shown). Scale bar, 50 μm.

Effects of Discontinuities in the ILM and Disruptions of MC Endfeet

Next, we asked whether disruptions in the ILM produces changes in MC organization. In wholemount preparations of WT retina, the ILM was a thin sheet laying on the retinal surface (Fig. 4A), and the endfoot of each MC appeared to encircle the neurons of the RGC layer, forming a regular array of processes across the surface of the ILM (Fig. 4C).[24] In contrast, in $\beta2^{-/-}\gamma3^{-/-}$ mice, the ILM was mostly absent (Fig. 4B), and MC endfeet did not show any particular relation to the RGC layer neurons (Fig. 4D). In particular, large regions of the vitreal surface were devoid of MC processes and, in other regions, the MC endfeet ended in a fibrotic tangle. In the radial sections (Figs. 4E, 4F), MC endfeet in the WT retinas terminated in a linear array of enlarged processes on the nidogen-positive ILM (Fig. 4E). In the $\beta2^{-/-}\gamma3^{-/-}$ retinas, the ILM was disrupted, and there were large regions of retina with no MC processes (Fig. 4F, arrowheads) or with processes terminating on the remaining BM found on blood vessels at the vitreal border (Fig. 4F, arrows).

MC differentiation was disrupted in $\beta2^{-/-}\gamma3^{-/-}$ retinas. In WT retinas, MCs expressed glutamine synthetase (GS) and were well organized, with cell bodies in the inner layer of the INL and radial processes extending apically and basally. Apically, MCs processes formed a band of tight junctions with each other and photoreceptors, generating the outer limiting membrane (OLM). GS levels continued to increase from P10 through P20 (Fig. 5), concomitant with the maturation of synaptic function in the OPL. In the $\beta2^{-/-}\gamma3^{-/-}$ retinas, MCs were markedly disrupted at P10 and P15. GS expression was reduced, and the organization of the cell was disrupted (Fig. 5). Specifically, the apical processes of MCs were disorganized and often expanded into the subretinal space (Fig. 5D, arrowheads), suggesting a disruption in OLM continuity. The basal endfeet formed fibrotic plaques that grew larger with age, particularly adjacent to vascular BMs (Fig. 5F). Patches of gliotic MCs, defined by upregulation of GFAP and assayed immunohistochemically, were seen in regions of retinal discontinuity (not shown).

Adherence of MCs to Laminin Substrates

We used a short-term in vitro binding assay to determine substrate specificity for rat MCs (rMC-1 cells). Binding was normalized to no-substrate conditions; rMC-1 cells showed an eightfold increase in adhesion to EHS laminin (which is a mixture of several native laminins, including those containing the $\beta2$ chain), as well as to poly-L-lysine (Fig. 6). MCs showed a significant binding preference (3.75-fold) for the laminin $\beta2$ short arm. This somewhat decreased affinity for $\beta2$ short arm over EHS laminins (3.75 vs. 8) is not surprising, given the lack of several cell-binding domains provided by the associated LG domains in the native α chains present in EHS laminins. Of note, the rMC-1 cells did not bind to full-length netrin-4, which has considerable amino acid identity with laminin β chains.[25] These data clearly demonstrate that MCs recognize and adhere to laminins in general and, in particular, the $\beta2$ chain.

Dystroglycan is reported to be a laminin receptor located on MC endfeet; thus, we used double immunostaining to study β-dystroglycan distribution and its colocalization with perlecan

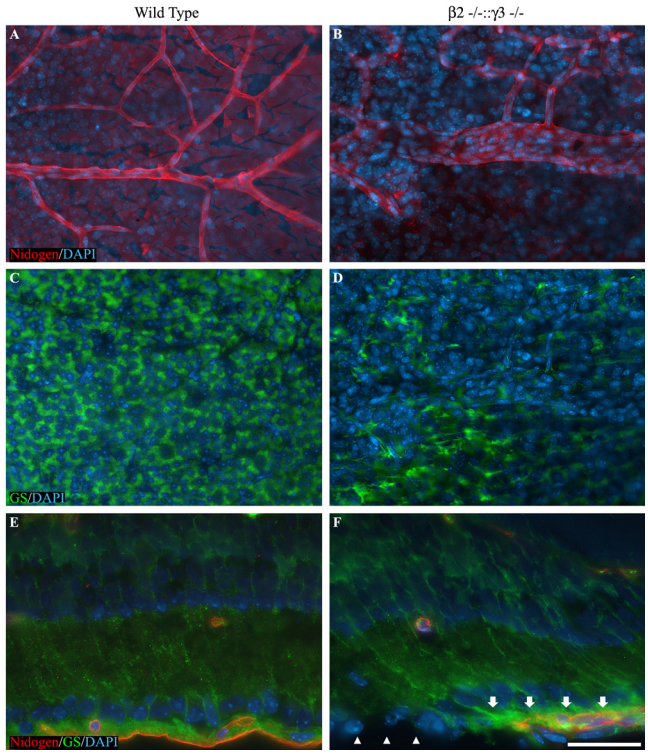

FIGURE 4. MC endfeet were disrupted where the ILM was discontinuous in the $\beta2^{-/-}\gamma3^{-/-}$ retina. The ILM was visualized by nidogen deposition (*red*), MCs by GS staining (GS; *green*), and cell nuclei with DAPI (*blue*). Wholemount preparations of the retina (**A–D**) and radial sections (**E**, **F**) were shown. (**A**) The ILM was a seen as a continuous sheet with overlaying blood vessels; (**B**) in the mutant retina, there was no apparent ILM, and vascular defects were present. (**C**) MC endfeet (*green* processes) formed a lattice-like network surrounding the cells (DAPI) of the ganglion cell layer. (**D**) This regular array of endfeet was disrupted in the laminin mutant. The relationship of MC endfeet and the ILM was best seen in radial sections (**E**, **F**); in WT, MCs were perfectly radial and their endfeet sat on the ILM surface, whereas in the mutant retina, large regions of the retina were devoid of MC endfeet (*arrowheads*) and MC processes deviated toward and adhered to the intact vascular BM (**E**, *arrows*). Scale bar: (**A–D**) 100 μm; (**E**, **F**) 50 μm.

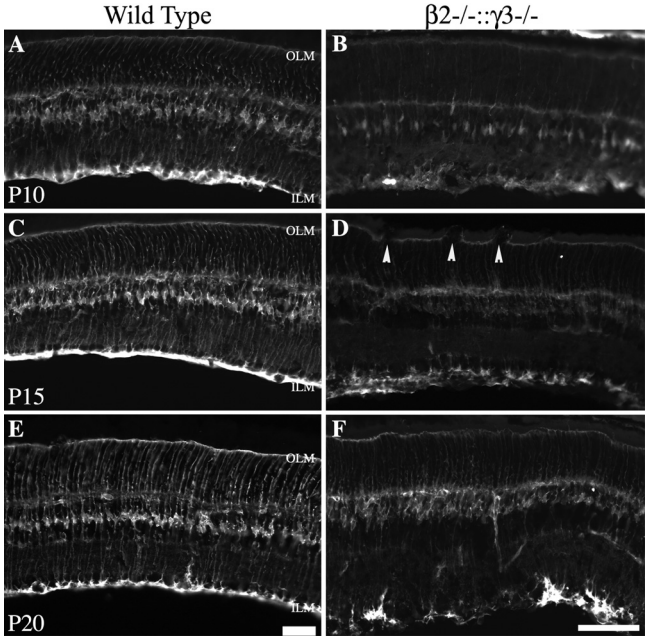

FIGURE 5. MC maturation in the $\beta2^{-/-}\gamma3^{-/-}$ retina was disrupted throughout development. GS was used to label MCs during development. (**A**, **C**, **E**) Radial sections of WT retina; (**B**, **D**, **F**) sections of age-matched mutant retinas. GS expression in the mutant retina lagged behind that of the WT (**B** vs. **A**). Moreover, MC morphology was disrupted over the whole age range. Early in development (**B**), the apparent density of cells was lower and the MC endfeet did not form a regular array. Later (**D**), apical processes from the MCs invaded the subretinal space at points where the OLM was disrupted (*arrows*). As development proceeded (**F**), fibrotic tangles on the vitreal surface became large, whereas the OLM remained disrupted and discontinuous. Scale bar, 50 μm.

in WT and the $\beta2^{-/-}\gamma3^{-/-}$ retinas. In agreement with previous reports,[22] in WT retina, we found β-dystroglycan immunoreactivity in the basal RPE, in the OPL, and at the ILM and surrounding blood vessels. In the mutant retinas, β-dystroglycan, and perlecan immunoreactivities were lost in the ILM, whereas co-staining appeared normal at Bruch's membrane and the vascular BMs (Fig. 7F, arrows).

Ultrastructural Defects in Laminin-Null Retinas

Several abnormalities in the ultrastructure of BMs and the attached cells were apparent in the $\beta2^{-/-}\gamma3^{-/-}$ retina (Fig. 8). Bruch's membrane was thickened and showed some disorganization in the arrays of collagen and elastin fibrils (Figs. 8A, 8B). The RPE varied from healthy-appearing cells to hyperplastic cells, with loss of pigment, enlarged vacuoles, and disruptions in the basal processes (Figs. 8C, 8D). Photoreceptor outer segments were shorter and less organized; ectopic cells were found in the subretinal space (Figs. 8E, 8F). The adherens junctions forming the OLM were irregular; in many regions they were completely absent (Figs. 8G, 8H). In the OPL, disruptions of rod photoreceptor synapses were apparent in the $\beta2^{-/-}\gamma3^{-/-}$ retina (Figs. 8I, 8J). A significant number of ribbon synapses were dysmorphic in the $\beta2^{-/-}\gamma3^{-/-}$ retinas; 30.7% of all ribbons were floating free in the cytoplasm of the rod terminal in the mutant compared with 10% in the WT retinas (n = 189, and 130, respectively). In the WT, 88.2% of the ribbon synapses in the OPL showed normal functional relationship with two or three postsynaptic contacts (dyads or triads, respectively) versus only 67.7% in the mutant retinas. These data are nearly identical with those reported for the $\beta2^{-/-}\gamma3^{+/+}$ animal, in which a profound disruption of synaptic integrity was noted.[12]

Last, consistent with the light microscopic observations, the vitreal surface of the $\beta2^{-/-}\gamma3^{-/-}$ retina was markedly dysmorphic. The normal trilaminate structure of the ILM (Fig. 8K) was absent, and the remaining portions were loosely adherent to the retina (Fig. 8L). We observed processes of presumed MCs sprouting into the vitreal cavity (Fig. 8L) similar to the events of proliferative vitreoretinopathy. Consistent with the results reported thus far in the article, these data suggest that MCs adhere to ILM laminins.

Disruption of the Laminar Arrangement in the Laminin $\beta2\gamma3$ Chain-Deficient Retina

Neuronal differentiation was examined in sections of P20 WT and mutant retinas with a panel of immunohistochemical markers (Fig. 9; Table 1). In the $\beta2^{-/-}\gamma3^{-/-}$ retinas, we selected both regions with relatively normal organization and regions with impaired lamination for comparison; shown in Figure 9 were regions of moderate disorganization. Several generalizations can be made. First, all classes of cells appeared to be present. Second, the fundamental layered organization of the retina was largely intact. Third, the polarity of the cells was largely intact. The photoreceptors were aligned well and the rod bipolar cells and amacrine cells were properly oriented.

Nevertheless, within individual cell types, several disruptions in organization were found. As noted earlier, rosettes formed in the outer retina, consisting largely of photoreceptors. These ectopic cells were polarized around an ectopic subretinal space,

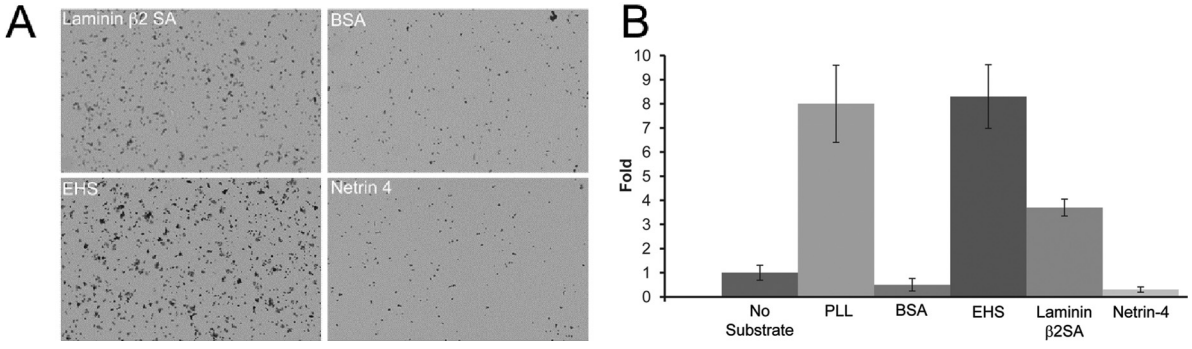

FIGURE 6. MCs showed preferential attachment to laminin substrates. Short-term adhesion assays were performed on glass coverslips (no substrate) or glass coverslips coated with poly-L-lysine (PLL), EHS laminin (EHS), laminin $\beta2$ short arm (laminin $\beta2$ SA), bovine serum albumin (BSA), or full-length netrin-4 (netrin 4). (**A**) Representative assays with EHS, $\beta2$ SA, BSA, and netrin-4 are shown. MCs adhered to the laminin substrates (EHS, $\beta2$SA) but not to the closely related netrin-4 or BSA. (**B**) In a histogram analysis of all conditions, rMC-1 cells exhibited a preference for laminin substrates.

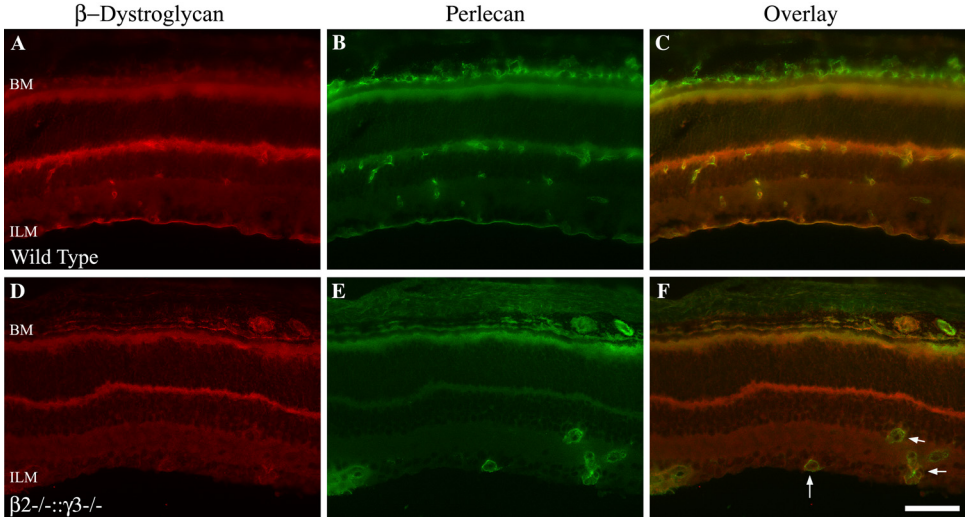

FIGURE 7. β-Dystroglycan expression was disrupted in the MC endfeet. (**A–C**) Radial sections of WT and (**D–F**) laminin-deficient retina; perlecan was used as a BM marker in this study. Normally, β-dystroglycan was expressed in juxtaposition with retinal BMs. (**A–C**) Particularly noteworthy was the distribution surrounding the vascular BM and in the MC endfeet at the ILM (**A**; *yellow* in **C**). In the laminin-deficient retina, β-dystroglycan disappeared from the retinal surface but continued to surround the vascular BM (**D**, **E**, *arrows*). ILM continuity was disrupted specifically as perlecan staining disappeared from the mutant ILM, but it was present in Bruch's membrane and the vascular BM (**E**). Scale bar, 50 μm.

which was continuous with the normal subretinal space (Fig. 9B, arrows). These ectopic photoreceptors made outer segments and transported opsin into them (Fig. 9B and Supplementary Fig. S1, http://www.iovs.org/cgi/content/full/51/3/1773/DC1). In addition, rhodopsin was not confined to the outer segments in either normally positioned photoreceptors or photoreceptors within

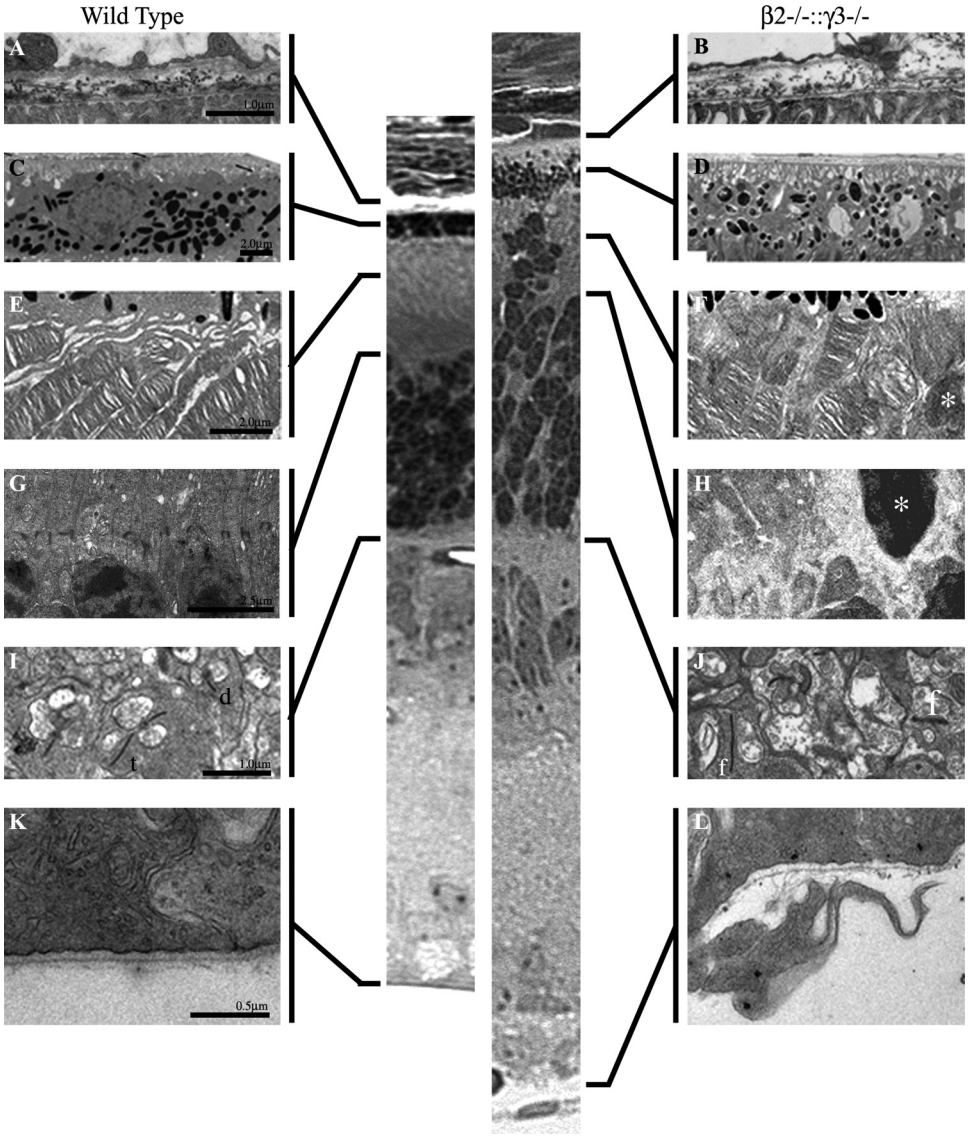

FIGURE 8. Electron micrographs revealed ultrastructural abnormalities across the retina in the $\beta2^{-/-}\gamma3^{-/-}$ retina. Ultrastructural analysis of WT and mutant retinas, the mutant retina displayed several morphologic disruptions compared with the control. Retinas from WT animals are shown in the left column (**A**, **C**, **E**, **G**, **I**, **K**); mutant retinas are shown in the right column (**B**, **D**, **F**, **H**, **J**, **L**). In the middle panels are low-power images of sections from WT and mutant retina for orientation. (**A**, **B**) In the mutant, Bruch's membrane was thickened and the collagen and elastin fibril organization was disrupted. (**C**, **D**) Mutant RPE was markedly vacuolated, and there were disruptions in the basal processes (not fully illustrated). (**E**, **F**) The outer segments in the mutant were disorganized and misaligned, with shorter disc membranes. (**G**, **H**) In the WT, the OLM was formed from a series of zonulae adherens. In the mutant, these junctions were disrupted; ectopic photoreceptor nuclei (✻ in **F** and **H**; see also the orientation figure) were found at these sites of discontinuities. (**I**, **J**) There was considerable disruption of synaptic organization in the OPL of the mutant retina numerous floating ribbons (f) were found in the mutant. (**K**, **L**) MC processes sprouted into the vitreous cavity where the ILM was disrupted.

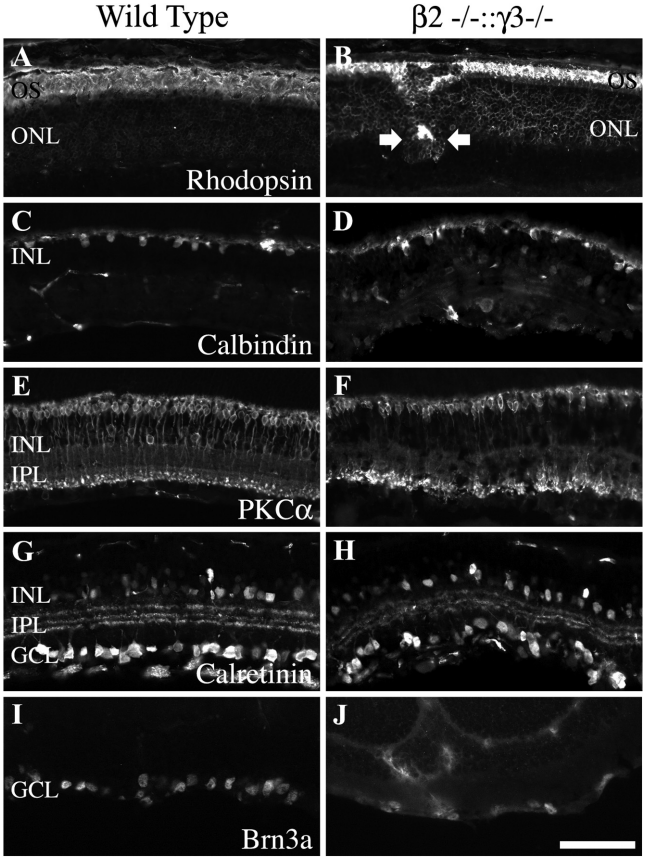

FIGURE 9. Retinal cells differentiate, but their laminar arrangement was disrupted in the laminin-deficient retina. Radial sections of WT (**A**, **C**, **E**, **G**, **I**) and mutant (**B**, **D**, **F**, **H**, **J**) P20 retina were examined for a variety of cell-specific markers (as indicated). All major cell types were present in mutant retinas, but their lamination was disrupted in patches (**D**, **H**, **J**). This disruption was most striking in the photoreceptors, which gathered in spheroid clusters with their outer segment oriented toward the center (**B**, rosette formation, *arrows*). Rhodopsin also showed a marked delocalization, staining the photoreceptor bodies (see Supplementary Fig. S1, http://www.iovs.org/cgi/content/full/51/3/1773/DC1). Finally, there were variable irregularities in the strict arrangement and laminar patterning of horizontal (**C**, **D**), bipolar (**E**, **F**), amacrine (**G**, **H**), and ganglion (**I**, **J**) cells and their processes. Scale bar, 50 μm.

rosettes. Rather, there was significant rhodopsin immunoreactivity in the cell bodies of photoreceptors, and thus it appeared throughout the ONL (Fig. 9B, Supplementary Fig. S1).

The organization of the rod bipolar cell terminals in the IPL appeared to be disrupted (Figs. 9E, 9F). In WT retinas, these cells ended in a tight band of terminals at the distalmost portions of the IPL (Fig. 9E); in the $\beta2^{-/-}\gamma3^{-/-}$ retina, this band was widened and disorganized (Fig. 9F). Amacrine cells and RGCs, visualized with calretinin immunohistochemistry, revealed disruptions in cell positioning and in the characteristic trilaminate staining of the IPL (compare Fig. 9G with Fig. 9H). We have published a study of the effect on the dopaminergic system in this retina.[14] The ganglion cell layer was severely affected. RGC bodies were not properly organized in the RGC layer, with many RGCs extruding into the vitreous (compare Fig. 9J with Fig. 9I).

Effect of Laminin $\beta2\gamma3$ Chain Deficiency on ERG a- and b-Waves

The physiological consequences of laminin $\beta2$ and $\gamma3$ ablation were analyzed in an electrophysiological approach. Figure 10 shows representative ERG recordings from P18 WT and $\beta2^{-/-}\gamma3^{-/-}$ mice in response to flash stimuli delivered after prolonged dark adaptation. It was immediately evident that the postsynaptic responses (b-wave) were as severely disrupted in the $\beta2^{-/-}\gamma3^{-/-}$ animals (Figs. 10A, 10B) as they were in the $\beta2^{-/-}\gamma3^{+/+}$ animals.[12] However, unlike in the $\beta2^{-/-}\gamma3^{+/+}$ mutants, the photoreceptor-generated currents (a-wave) in the $\beta2^{-/-}\gamma3^{-/-}$ animals were also disrupted. In the $\beta2^{-/-}\gamma3^{-/-}$ animals, the mean amplitudes of a-waves were reduced to ~38% of control values, whereas the b-waves were reduced to ~45% of the control (Figs. 10A, 10B). In addition to a reduction in the a-wave amplitude, the implicit time is increased from 30.2 ms in WT retinas to 35.7 ms in $\beta2^{-/-}\gamma3^{-/-}$ retinas; the implicit time of the b-wave wave was largely unaltered (80.5 vs. 81.3 ms). Finally, there was a dramatic reduction in a-wave sensitivity in the compound nulls (Fig. 10C; ~1.75-log unit shift) and the responsivity of both a- and b-waves was drastically reduced (Figs. 10C, 10D).

It is also clear that cone function is diminished in $\beta2^{-/-}\gamma3^{-/-}$ retinas. At higher intensity flashes, oscillations in the b-wave are commonly attributed to cone-activation.[26] These oscillations are diminished in the $\beta2^{-/-}\gamma3^{-/-}$ retinas but not ablated, suggesting that cone function may be preserved (Fig. 10A, top left, compare WT and nulls). The dramatic reduction in the b-wave amplitude is most likely the result of the disruption of synaptic integrity in these animals (see the EM results described earlier), which was also seen in the $\beta2^{-/-}\gamma3^{+/+}$ retina.[12] Disruptions in MC function may also contribute to this reduction in the compound-null animal.

DISCUSSION

A key step in retinal development involves the functional subdivision of the tissue, not only the differentiation of glial and neural cell types, but also the ability to form different cell shapes and to subdivide the tissue into functionally distinct compartments. The resultant multilaminated structure is dependent on the adequate establishment of apical–basal cell polarity. The retina, like the rest of the CNS, is derived from the neural tube with origins in the ectoderm. In ectodermally derived tissues, apical–basal polarity is conferred by the adhesion of epithelial cells to the BM. Loss of BM integrity or misexpression of BM components has profound developmental consequences and, in adulthood, disruptions in BM integrity can lead to a variety of diseases, including kidney dysfunction, muscular dystrophies, and metastatic cancer. Disruptions in genes encoding laminin, ECM receptors (integrin, dystroglycan), their signaling molecules (ILK, FAK), or cytomatrix molecules (dystrophin) cause cortical and retinal dysplasia in animal models[27–35] and humans.[36]

Laminins are dynamically regulated during development, and the regulation of their expression is complex. However, several important generalizations about the role of laminins in development have emerged. First, is the primacy of laminin in BM formation and stability. The laminin trimer, $\alpha1\beta1\gamma1$ is expressed early, and the deletion of *Lamc1* (the $\gamma1$ gene) results in preimplantation lethality[2] during epiblast formation. The addition of exogenous laminin to the *Lamc1*-null embryoid bodies restores BM formation and development through gastrulation.[37,38] Laminin-mediated assembly of the BM proceeds as follows: (1) binding of laminin via the LG domains to cell surface sulfated glycolipids; and (2) polymerizing via their LN terminals and incorporation of other ECM molecules to the nascent laminin polymer including collagen and HSPGs.[39] Another generalization that can be made is that early laminin isoforms are replaced in many tissues by different isoforms in a tissue-specific manner.[40]

Herein, we describe a series of histogenic effects in the retina, which arise from a common problem: the loss of integrity of a single BM—the ILM. We demonstrate that both $\beta2$- and

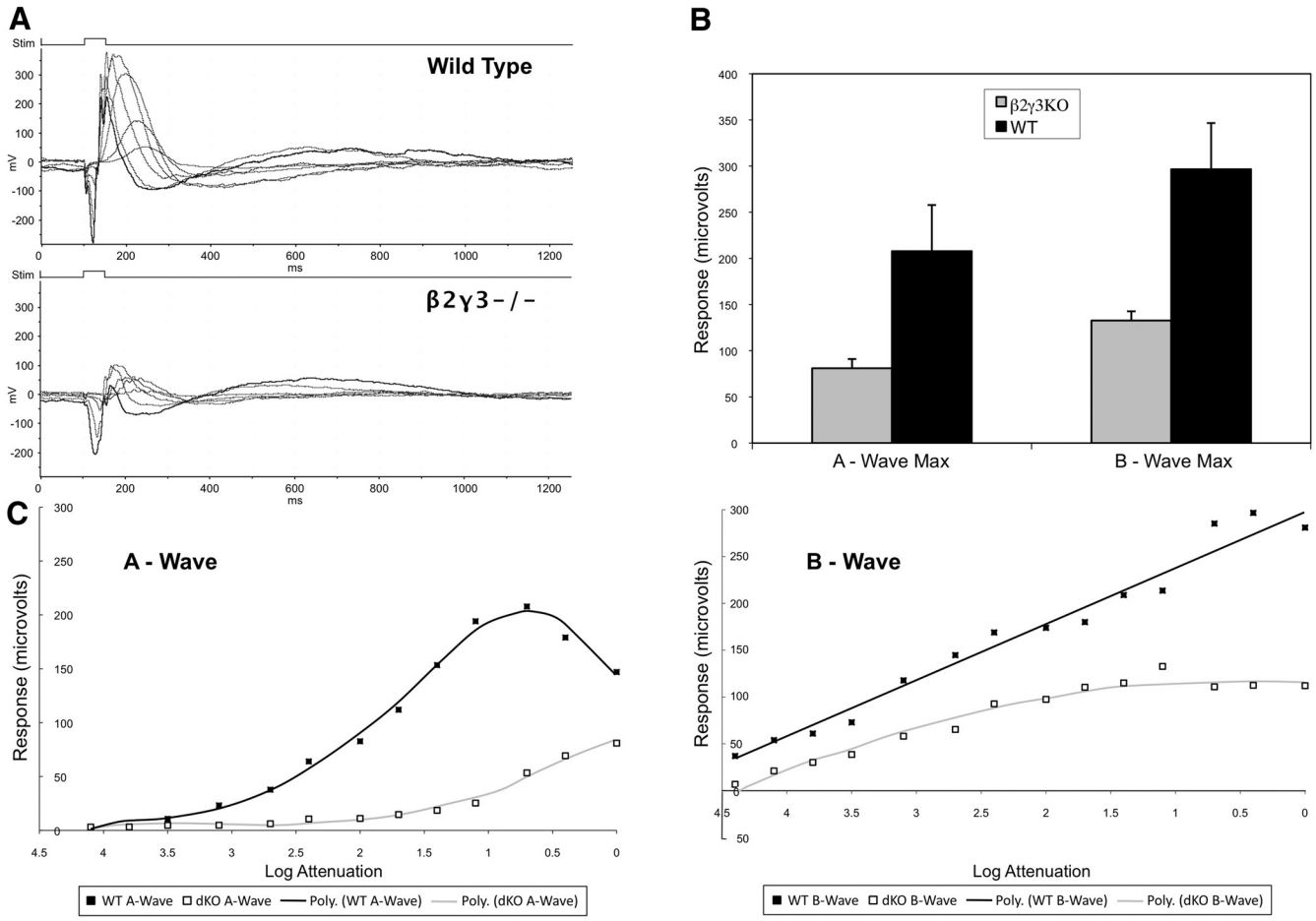

FIGURE 10. ERGs demonstrated profound dysfunction in photoreceptor transduction and output in the mutant retina. (**A**) Representative ERGs from WT (*top*) and laminin-deficient mice (*bottom*) are shown; the a- and b-wave amplitudes were reduced at all light intensities. (**B**) Histograms of a- and b-waves of all animals studied. (**C**) Response–intensity curves for a- and b-waves in WT and mutant mice; regression lines are drawn through the data points. In addition to profound reduction in the a-wave amplitude, the a-wave threshold was elevated considerably. The disruptions of the b-wave were consistent with the ultrastructural disruptions of the synapse in this mouse and in the $\beta2^{-/-}$ mouse.[12]

γ3-containing laminins are components of the ILM and are essential for the stabilized assembly of the ILM; other BMs—vascular and Bruch's—are intact. The need for β2- and γ3-containing laminins in the ILM apparently arises late in development, as the central ILM is intact and formed in these animals, whereas the more peripheral ILM is disrupted. This situation is reminiscent of the temporal regulation of laminin expression in epithelial systems where a shift in isoforms precedes and parallels histogenic maturation.[41,42]

Multiple sources of ILM laminins are possible and include the lens, the neural retina (Müller and neuroepithelial cells), and the ciliary body.[43] As development proceeds and the vitreous body expands, distant sources of laminin for ILM synthesis seem unlikely. Thus, it may be that retinal sources become increasingly more important for ILM synthesis with advancing age.

The single deletion of either *Lamb2* or *Lamc3* alone minimally disrupts the ILM. How then does their combined deletion so profoundly disrupt the ILM formation with apparent specificity? As the β3 and γ2 chains appear to be exclusive partners, only β1 and γ1 laminin chains can compensate for the loss of β2 and γ3, respectively. It is now emerging that the β2 and γ3 chains have some unique binding properties. For example, the presence of a γ3 chain in a laminin isoform reduces that isoform's apparent integrin binding. Similarly, β2 and β1 also have differential binding affinities for some integrins.[44,45] Moreover, the dynamics of laminin polymerization, which occurs as a result of the interaction among the LN (N-terminals) of the molecules, is no doubt different among the chains.[46] Thus, the biological properties of laminin β1- and γ1-containing laminins are fundamentally different from those of β2- and γ3-containing ones.

The alterations during retinal histogenesis, as described for the $\beta2^{-/-}\gamma3^{-/-}$ retina, are referred to as dysplasia (i.e., disturbances in development that result in the disruption of the normal tissue architecture).[47,48] The mechanisms that regulate normal retinal lamination are coming under increasing study.[49,50] A clear concept is emerging that the mechanisms of lamination and cell fate adoption are genetically separable. Retinal cell differentiation and lamination appear to proceed in the same time window, but use separate molecular mechanisms.[51,52] Our results are consistent with these observations: The deletion of both the β2 and γ3 chains of laminin, although it disrupts dendritogenesis,[14] does not affect cell fate.

Moreover, although the β2- and γ3-deficient retina showed some anomalies at P0, the most dramatic dysplasia occurred during the second postnatal week, when rod photoreceptors and MCs were being born and differentiating. MCs were highly polarized with distinct subcellular compartments. A series of tight junctions were found at the apical surface of the MC; these were disrupted in the $\beta2^{-/-}\gamma3^{-/-}$ mouse. Similarly, there were receptor complexes present at the basal endfoot

that were disrupted also in the $\beta2^{-/-}\gamma3^{-/-}$ mouse. MCs span the entire thickness of the neural retina, establishing morphologic and functional interactions with all retinal neurons. They were also intimately related with both limiting membranes as well as with the synaptic layers. Several studies have suggested that MC disruption causes disorganization of the normal retinal layering.[53–59] The laminin receptor dystroglycan is expressed in MCs and mediates MC adhesion and migration as well as macromolecular clustering of the transport molecules aquaporin and Kir4.1 channels.[60] In reaggregated cultures of retinal neurons, the correct polarity of retinal layers is associated with the release of laminin by co-cultured RPE cells.[61] It seems reasonable to presume that BM proteins, laminin in particular, provide critical polarity cues in organizing the MCs.

In the $\beta2^{-/-}\gamma3^{-/-}$ retina, the integrity of the ILM was disrupted, which was accompanied by the loss of expression of β-dystroglycan (the transmembrane component of the dystroglycan complex) at the MC endfeet. This effect suggests that an intact ILM is necessary for proper assembly and/or localization of β-dystroglycan at the MC endfeet. The resulting lack of interaction between ECM proteins in the BM and β-dystroglycan at the endfeet of MCs may result in an abnormal maturation of these cells, preventing them from establishing adequate contacts with other cells, thus leading to retinal disorganization. In this regard, retinas of mice with mutations in α-dystroglycan, the ligand-binding component of the dystroglycan complex, are disorganized, similar to that in the $\beta2^{-/-}\gamma3^{-/-}$ mouse.[62] Deletions of integrins α3 and α6 produce retinal dysplasia as well. All these studies suggest that adhesion to the BM is critical for retinal histogenesis. Further support comes from the work of Chen and Nathans,[63] who showed that outer retinal dysplasia in the rd7 mouse is probably the result of specific disruptions of cone photoreceptors with MCs and the ECM.[63] The results reported here identify β2 and γ3 laminins as key organizers of the ILM and implicated them as critical molecules for MC adhesion to the ILM.

In addition to the profound dysplasia, β2- and γ3-deficient retinas showed abnormalities in photoreceptor morphogenesis (i.e., shorter and disorganized outer segments and detached or floating synaptic ribbons). There was also a disorganization of opsin targeting, resulting in misexpression of opsin in the ONL. Such delocalization of opsin is a common theme during photoreceptor injury and degeneration such as that in retinal detachment.[64] It remains to be determined whether laminins contribute directly to outer segment stabilization or these structural effects on the photoreceptor are mediated through MCs. These morphologic photoreceptor abnormalities phenocopy the effects of the laminin β2 chain-deficient retina[12]; however, there were functional differences in the two mice as measured by the ERG. Unlike the $\beta2^{-/-}$ single mutant, the amplitude of the a-wave was reduced, and the implicit time was increased in the $\beta2^{-/-}\gamma3^{-/-}$ mouse, suggesting profound dysfunction in the signal transduction process. This disruption may reflect a more profound intrinsic disruption of photoreceptor morphogenesis, in that the outer segments are shortened in both mutants.[12] Another possibility is that the photon capture rate in $\beta2^{-/-}\gamma3^{-/-}$ retinas is impaired by MC disorganization. MCs have been shown to act as effective light guides in normal retinas.[65] Given the profound geometric rearrangement in the $\beta2^{-/-}\gamma3^{-/-}$ animal and the near complete disruption of the array of MC endfeet, this light-gathering ability would be greatly impaired in these animals.

The $\beta2^{-/-}\gamma3^{-/-}$ and $\beta2^{-/-}\gamma3^{+/+}$ mice[12] both have profound reductions in the b-wave, which is accompanied by morphologic failure in synaptogenesis. This synaptic disruption may explain another aspect of the $\beta2^{-/-}\gamma3^{-/-}$ phenotype. MCs are responsible for recycling glutamate to glutamine, via GS. GS expression is inducible and regulated by glutamate release.[66] The decrease in GS seen in the compound null is consistent with a disruption in synaptic function and the reduction of the b-wave.

Taken together, these results suggest that the β2 and γ3 chains of laminin: (1) are critical for the normal organization of BMs and tissue histogenesis in the CNS and (2) are essential for normal polarity and maturation of MCs. These studies may be relevant to our understanding of the pathobiology of MCs and may provide the basis for ECM-targeted therapies.

Acknowledgments

The authors thank Paul Witkovsky for critical reading of an earlier version of the manuscript and Galina Bachay for technical help.

References

1. Aumailley M, Bruckner-Tuderman L, Carter WG, et al. A simplified laminin nomenclature. *Matrix Biol.* 2005;24:326–332.
2. Smyth N, Vatansever HS, Murray P, et al. Absence of basement membranes after targeting the LAMC1 gene results in embryonic lethality due to a failure of endoderm differentiation. *J Cell Biol.* 1999;144:151–160.
3. Yurchenco PD, Amenta PS, Patton BL. Basement membrane assembly, stability and activities observed through a developmental lens. *Matrix Biol.* 2004;22:521–538.
4. Kramer JM. Basement membranes. *WormBook.* 2005;30:1–15.
5. Nelson CM, Bissell MJ. Of extracellular matrix, scaffolds, and signaling: tissue architecture regulates development, homeostasis, and cancer. *Annu Rev Cell Dev Biol.* 2006;22:287–309.
6. Burgeson RE, Chiquet M, Deutzmann R, et al. A new nomenclature for the laminins. *Matrix Biol.* 1994;14:209–211.
7. McGowan KA, Marinkovich MP. Laminins and human disease. *Microsc Res Tech.* 2000;51:262–279.
8. Zenker M, Aigner T, Wendler O, et al. Human laminin beta2 deficiency causes congenital nephrosis with mesangial sclerosis and distinct eye abnormalities. *Hum Mol Genet.* 2004;13:2625–2632.
9. Colognato H, ffrench-Constant C, Feltri ML. Human diseases reveal novel roles for neural laminins. *Trends Neurosci.* 2005;28:480–486.
10. Miner JH, Go G, Cunningham J, Patton BL, Jarad G. Transgenic isolation of skeletal muscle and kidney defects in laminin beta2 mutant mice: implications for Pierson syndrome. *Development.* 2006;133:967–975.
11. Libby RT, Champliaud MF, Claudepierre T, et al. Laminin expression in adult and developing retinas: evidence of two novel CNS laminins. *J Neurosci.* 2000;20:6517–6528.
12. Libby RT, Lavallee CR, Balkema GW, Brunken WJ, Hunter DD. Disruption of laminin β2 chain production causes alterations in morphology and function in the CNS. *J Neurosci.* 1999;19:9399–9411.
13. Noakes PG, Miner JH, Gautam M, Cunningham JM, Sanes JR, Merlie JP. The renal glomerulus of mice lacking s-laminin/laminin beta 2: nephrosis despite molecular compensation by laminin beta 1. *Nat Genet.* 1995;10:400–406.
14. Dénes V, Witkovsky P, Koch M, Hunter DD, Pinzón-Duarte G, Brunken WJ. Laminin deficits induce alterations in the development of dopaminergic neurons in the mouse retina. *Vis Neurosci.* 2007;24:549–562.
15. Barnstable CJ. Monoclonal antibodies which recognize different cell types in the rat retina. *Nature.* 1980;286:231–235.
16. Haverkamp S, Wässle H. Immunocytochemical analysis of the mouse retina. *J Comp Neurol.* 2000;424:1–23.
17. Xiang M, Zhou L, Macke JP, Yoshioka T, et al. The Brn-3 family of POU-domain factors: primary structure, binding specificity, and expression in subsets of retinal ganglion cells and somatosensory neurons. *J Neurosci.* 1995;15:4762–4785.
18. Bignami A, Dahl D. The radial glia of Müller in the rat retina and their response to injury: an immunofluorescence study with antibodies to the glial fibrillary acidic (GFA) protein. *Exp Eye Res.* 1979;28:63–69.
19. Ito M, Nakashima M, Tsuchida N, Imaki J, Yoshioka M. Collagen IV Histogenesis of the intravitreal membrane and secondary vitreous in the mouse. *Invest Ophthalmol Vis Sci.* 2007;48:1923–1930.
20. Halfter W, Willem M, Mayer U. Basement membrane-dependent survival of retinal ganglion cells. *Invest Ophthalmol Vis Sci.* 2005;46:1000–1009.

21. Soulintzi N, Zagris N. Spatial and temporal expression of perlecan in the early chick embryo. *Cells Tissues Organs.* 2007;186:243–256.
22. Montanaro F, Carbonetto S, Campbell KP, Lindenbaum M. Dystroglycan expression in the wild type and mdx mouse neural retina: synaptic colocalization with dystrophin, dystrophin-related protein but not laminin. *J Neurosci Res.* 1995;42:528–538.
23. Sarthy VP, Brodjian SJ, Dutt K, Kennedy BN, French RP, Crabb JW. Establishment and characterization of a retinal Müller cell line. *Invest Ophthalmol Vis Sci.* 1998;39:212–216.
24. Dreher Z, Robinson SR, Distler C. Müller cells in vascular and avascular retinas: a survey of seven mammals. *J Comp Neurol.* 1992;323:59–80.
25. Koch M, Murrell JR, Hunter DD, et al. A novel member of the netrin family, beta-netrin, shares homology with the beta chain of laminin: identification, expression, and functional characterization. *J Cell Biol.* 2000;151:221–234.
26. Peachey NS, Goto Y, al-Ubaidi MR, Naash MI. Properties of the mouse cone-mediated electroretinogram during light adaptation. *Neurosci Lett.* 1993;162:9–11.
27. Costell M, Gustafsson E, Aszódi A, et al. Perlecan maintains the integrity of cartilage and some basement membranes. *J Cell Biol.* 1999;147:1109–1122.
28. Graus-Porta D, Blaess S, Senften M, et al. Beta1-class integrins regulate the development of laminae and folia in the cerebral and cerebellar cortex. *Neuron.* 2001;31:367–379.
29. Halfter W, Dong S, Yip YP, Willem M, Mayer U. A critical function of the pial basement membrane in cortical histogenesis. *J Neurosci.* 2002;22:6029–6040.
30. Moore SA, Saito F, Chen J, et al. Deletion of brain dystroglycan recapitulates aspects of congenital muscular dystrophy. *Nature.* 2002;418:422–425.
31. Beggs HE, Schahin-Reed D, Zang K, et al. FAK deficiency in cells contributing to the basal lamina results in cortical abnormalities resembling congenital muscular dystrophies. *Neuron.* 2003;40:501–514.
32. Pöschl E, Schlötzer-Schrehardt U, Brachvogel B, Saito K, Ninomiya Y, Mayer U. Collagen IV is essential for basement membrane stability but dispensable for initiation of its assembly during early development. *Development.* 2004;131:1619–1628.
33. Niewmierzycka A, Mills J, St-Arnaud R, Dedhar S, Reichardt LF. Integrin-linked kinase deletion from mouse cortex results in cortical lamination defects resembling cobblestone lissencephaly. *J Neurosci.* 2005;25:7022–7031.
34. Semina EV, Bosenko DV, Zinkevich NC, et al. Mutations in laminin alpha 1 result in complex, lens-independent ocular phenotypes in zebrafish. *Dev Biol.* 2006;299:63–77.
35. Biehlmaier O, Makhankov Y, Neuhauss SC. Impaired retinal differentiation and maintenance in zebrafish laminin mutants. *Invest Ophthalmol Vis Sci.* 2007;48:2887–2894.
36. Mochida GH, Walsh CA. Genetic basis of developmental malformations of the cerebral cortex. *Arch Neurol.* 2004;61:637–640.
37. Li S, Harrison D, Carbonetto S, et al. Matrix assembly, regulation, and survival functions of laminin and its receptors in embryonic stem cell differentiation. *J Cell Biol.* 2002;157:1279–1290.
38. Yurchenco PD, Wadsworth WG. Assembly and tissue functions of early embryonic laminins and netrins. *Curr Opin Cell Biol.* 2004;16:572–579.
39. McKee KK, Harrison D, Capizzi S, Yurchenco PD. Role of laminin terminal globular domains in basement membrane assembly. *J Biol Chem.* 2007;282:21437–24147.
40. Miner JH, Yurchenco PD. Laminin functions in tissue morphogenesis. *Annu Rev Cell Dev Biol.* 2004;20:255–284.
41. Miner JH, Patton BL, Lentz SI, et al. The laminin alpha chains: expression, developmental transitions, and chromosomal locations of alpha1–5, identification of heterotrimeric laminins 8-11, and cloning of a novel alpha3 isoform. *J Cell Biol.* 1997;137:685–701.
42. Mahoney ZX, Stappenbeck TS, Miner JH. Laminin alpha 5 influences the architecture of the mouse small intestine mucosa. *J Cell Sci.* 2008;121:2493–2502.
43. Halfter W, Dong S, Dong A, Eller AW, Nischt R. Origin and turnover of ECM proteins from the inner limiting membrane and vitreous body. *Eye.* 2008;22:1207–1213.
44. Taniguchi Y, Ido H, Sanzen N, et al. The C-terminal region of laminin β chains modulates the integrin binding affinities of laminins. *J Biol Chem.* 2009;284:7820–7831.
45. Ido H, Ito S, Taniguchi Y, et al. Laminin isoforms containing the gamma3 chain are unable to bind to integrins due to the absence of the glutamic acid residue conserved in the C-terminal regions of the gamma1 and gamma2 chains. *J Biol Chem.* 2008;283:28149–28157.
46. Schneiders FI, Maertens B, Böse K, et al. Binding of netrin-4 to laminin short arms regulates basement membrane assembly. *J Biol Chem.* 2007;282:23750–23758.
47. Lahav M, Albert DM, Wyand S. Clinical and histopathologic classification of retinal dysplasia. *Am J Ophthalmol.* 1973;75:648–667.
48. Whiteley HE. Dysplastic canine retinal morphogenesis. *Invest Ophthalmol Vis Sci.* 1991;32:1492–1498.
49. Kay JN, Roeser T, Mumm JS, et al. Transient requirement for ganglion cells during assembly of retinal synaptic layers. *Development.* 2004;131:1331–1342.
50. Mumm JS, Williams PR, Godinho L, et al. In vivo imaging reveals dendritic targeting of laminated afferents by zebrafish retinal ganglion cells. *Neuron.* 2006;52:609–621.
51. Godinho L, Mumm JS, Williams PR, et al. Targeting of amacrine cell neurites to appropriate synaptic laminae in the developing zebrafish retina. *Development.* 2005;132:5069–5079.
52. Fu X, Sun H, Klein WH, Mu X. β-Catenin is essential for lamination but not neurogenesis in mouse retinal development. *Dev Biol.* 2006;299:424–437.
53. Rich KA, Figueroa SL, Zhan Y, Blanks JC. Effects of Müller cell disruption on mouse photoreceptor cell development. *Exp Eye Res.* 1995;61:235–248.
54. Dubois-Dauphin M, Poitry-Yamate C, de Bilbao F, Julliard AK, Jourdan F, Donati G. Early postnatal Müller cell death leads to retinal but not optic nerve degeneration in NSE-Hu-Bcl-2 transgenic mice. *Neuroscience.* 2000;95:9–21.
55. Dyer MA, Cepko CL. Control of Müller glial cell proliferation and activation following retinal injury. *Nat Neurosci.* 2000;3:873–880.
56. Jablonski MM, Iannaccone A. Targeted disruption of Müller cell metabolism induces photoreceptor dysmorphogenesis. *Glia.* 2000;32:192–204.
57. Kainz PM, Adolph AR, Wong KY, Dowling JE. Lazy eyes zebrafish mutation affects Müller glial cells, compromising photoreceptor function and causing partial blindness. *J Comp Neurol.* 2003;463:265–280.
58. Fisher SK, Lewis GP. Müller cell and neuronal remodeling in retinal detachment and reattachment and their potential consequences for visual recovery: a review and reconsideration of recent data. *Vision Res.* 2003;43:887–897.
59. Lunardi A, Cremisi F, Dente L. Dystroglycan is required for proper retinal layering. *Dev Biol.* 2006;290:411–420.
60. Fort PE, Sene A, Pannicke T, et al. Kir4.1 and AQP4 associate with Dp71- and utrophin-DAPs complexes in specific and defined microdomains of Müller retinal glial cell membrane. *Glia.* 2008;56:597–610.
61. Wolburg H, Willbold E, Layer PG. Müller glia endfeet, a basal lamina and the polarity of retinal layers form properly in vitro only in the presence of marginal pigmented epithelium. *Cell Tissue Res.* 1991;264:437–451.
62. Lee Y, Kameya S, Cox GA, et al. Ocular abnormalities in Large^{myd} and Large^{vls} mice, spontaneous models for muscle, eye, and brain diseases. *Mol Cell Neurosci.* 2005;30:160–172.
63. Chen J, Nathans J. Genetic ablation of cone photoreceptors eliminates retinal folds in the retinal degeneration 7 (rd7) mouse. *Invest Ophthalmol Vis Sci.* 2007;48:2799–2805.
64. Fisher SK, Lewis, G.P. Linberg KA, Verardo MR. Cellular remodeling in mammalian retina: results from studies of experimental retinal detachment. *Prog Retin Eye Res.* 2005;24:395–431.
65. Franze K, Grosche J, Skatchkov SN, et al. Müller cells are living optical fibers in the vertebrate retina. *Proc Natl Acad Sci U S A.* 2007;104:8287–8292.
66. Shen F, Chen B, Danias J, et al. Glutamate-induced glutamine synthetase expression in retinal Müller cells after short-term ocular hypertension in the rat. *Invest Ophthalmol Vis Sci.* 2004;45:3107–3112.